



Exploration of the Modern Application and International Promotion of Traditional Chinese Medicine Based on the Self-Assembly Mechanism of Traditional Chinese Medicine Formulas

Hao Shengjie^{1*}, Ma Jingjie¹, Wei Yanzhi¹, Wang Bingjie¹, Duo Lan²

1.Gansu Agricultural University 2.College of Grassland Agricultural Science and Technology, Lanzhou University, Lanzhou, China 730070

*Corresponding to: Hao Shengjie

Abstract: As an important part of traditional Chinese culture, traditional Chinese medicine embodies a unique theoretical system and application value. Studies have shown that the drug components in Chinese medicine formulas form complex molecular structures through self-assembly mechanisms, which can affect their pharmacodynamic properties. This study aims to explore the mechanism of self-assembly in Chinese medicine formulas, so as to promote the modernization and internationalization of Chinese medicine. In this paper, berberine-baicalin, the main component of *Coptis baicalensis* and *Scutellaria baicalensis* in traditional Chinese medicine, as an example, the differences and mechanisms of self-assembly caused by co-frying and physical mixtures are studied, and the relationship between the morphology of self-assembly and the antibacterial effect is revealed through various techniques. Studies have shown that their physical mixed forms are all nanofibers, and nanospheres in their co-decoction form can affect amino acid biosynthesis and metabolism in bacteria. These findings provide an experimental basis for the R&D and promotion of TCM formula granules, according to which we are expected to optimize the preparation method of drugs, improve efficacy, reduce adverse reactions, promote the TCM industry, and inject new vitality into its global dissemination and recognition.

Keywords: Traditional Chinese Medicine, Traditional Chinese Medicine Formula, Self-Assembly, Modern Application, International Promotion

1 RESEARCH BACKGROUND

1.1 RESEARCH IDEAS

In recent years, the research on the extraction of small molecule drugs from Chinese medicinal materials has entered a bottleneck stage due to problems such as poor selectivity and low bioavailability [1]. But at the same time, improving the clinical application of existing drugs through self-assembly has become one of the hot topics [2]. This carrier-free self-assembly enables drug repurposing, thereby increasing drug activity without creating new risks [3,4]. For example, rhubarb acid can directly self-assemble to form a sustained-release gel by non-covalent bonds such as $\pi - \pi$ stacking, thereby significantly enhancing its anti-neuroinflammatory activity. In addition, some clinical

nucleoside antitumor drugs can self-assemble into stable nanoparticles with few side effects and good efficacy. At present, our research has found that small molecule natural products can enhance activity or reduce toxicity after self-assembly. For example, berberine (BBR)-based self-assembly can form stable and carry free nanoparticles with good biocompatibility, which adhere to bacterial surfaces and increase drug concentrations in the local environment [5,6]. In contrast, BBR and aristolochic acid can block the toxic groups of aristolochic acid by self-assembly, forming linear heterogeneous supramolecules, thereby reducing the acute nephrotoxicity of aristolochic acid[7]. Based on these studies, self-assembly strategy is considered to be a new idea to improve the clinical efficacy and improve the toxicity of traditional Chinese medicines.

1.2 BACKGROUND



For thousands of years, traditional Chinese medicine has played a vital role in disease prevention and control; It has formed a unique TCM system and is an inseparable part of traditional Chinese culture[8]. As one of the new forms of traditional Chinese medicine formulas, Chinese medicine formula granules have been widely used because of their convenient transportation, simple taking method and controllable quality [9,10]. It has not only been popularized in China, but also promoted in Asian countries such as Japan and South Korea, and has gradually been accepted by the pharmaceutical market in Western countries such as the United Kingdom, the United States, and Germany [11]. At present, more than 700 kinds of Chinese herbal formula granules have been put into clinical use in China, with annual market sales of billions of dollars [12,13]. However, since the advent of modern formula granules, there has been an important point of controversy compared to thousands of years of traditional decoctions, due to the lack of a process of decoction of combined herbs in traditional Chinese medicine formula granules. Previous studies have shown that many chemical components of Chinese medicines undergo different physical and chemical changes during the decoction process [14,15]. For example, the decoction of White Tiger Soup contains nanoparticles of about 100 nm, which have a complex composition, which has a good antipyretic effect on lipopolysaccharide-induced rabbit fever models [16]. There are also nanoclusters of different sizes in Pueraria mirifica soup, the main components of which are puerarin, baicalin, berberine, etc. [17]. In summary, clinically, the decoction process produces self-assembly bodies, which affect the biological activity of traditional Chinese medicines; the self-assembly mechanism may help to improve the clinical efficacy of formulated granules.

1.3 PURPOSE OF THE STUDY

Coptis chinensis Franch (CR) and *Scullaria baicalensis* Georgi (SR) are clinically classic combinations of traditional Chinese medicine, originating from the Typhoid Miscellaneous Diseases. CR-SR can be used as a medicinal pair, and the combination can enhance the efficacy of each other, such as Huanglian detoxification soup, Kudzu Qianlian soup, and Lixin soup [18-

20]. At present, many studies have shown that there is a phenomenon of phytochemical self-assembly to form supramolecules during the co-frying process of CR-SR [21-23]. Our study found that both BBR and baicalin (BA) are the main components of CR-SR herbal pairs, which can interact to form spherical nanoclusters during co-frying, and self-assembly significantly improves the inhibitory ability of *Staphylococcus aureus* (S. aureus) compared with BBR [24]. Similar results have been demonstrated in other phytochemical self-assembly of decoctions of Chinese medicine [25]. Therefore, co-decoction of traditional Chinese medicines is one of the necessary conditions for the formation of phytochemical self-assembly, which can affect the clinical efficacy, while how the thermodynamic process of co-decoction affects the activity of self-assembly of traditional Chinese medicines has not been elucidated. At the same time, it has been reported that the self-assembly process and its morphology are not only related to the solvent type, pH value, and environmental concentration, but also the temperature is important [26-30].

1.4 RESEARCH RESULTS

Based on the main components of classical Chinese medicine CR/SR, we used self-assembly strategy to observe the morphological characteristics of nanoclusters and nanofibers formed by co-frying and physical mixtures, respectively. Using multispectral techniques, the spatial differences in the spatial configuration of self-assembled bodies between nanoclusters and nanofibers were elucidated. The relationship between these two types of self-assembly and biological activity was further discussed in the *Staphylococcus aureus* model. Through morphological observations of bacteria and RNA-seq testing, it was found that the enhanced activity of the nanogroups was attributed to their effects on the cell surface, further affecting the biosynthesis and metabolism of amino acids (Figure 1). These data show that the compound decoction may be beneficial to improve the antibacterial effect and provide a reliable scientific basis for improving the clinical efficacy of traditional Chinese medicine formula granules.

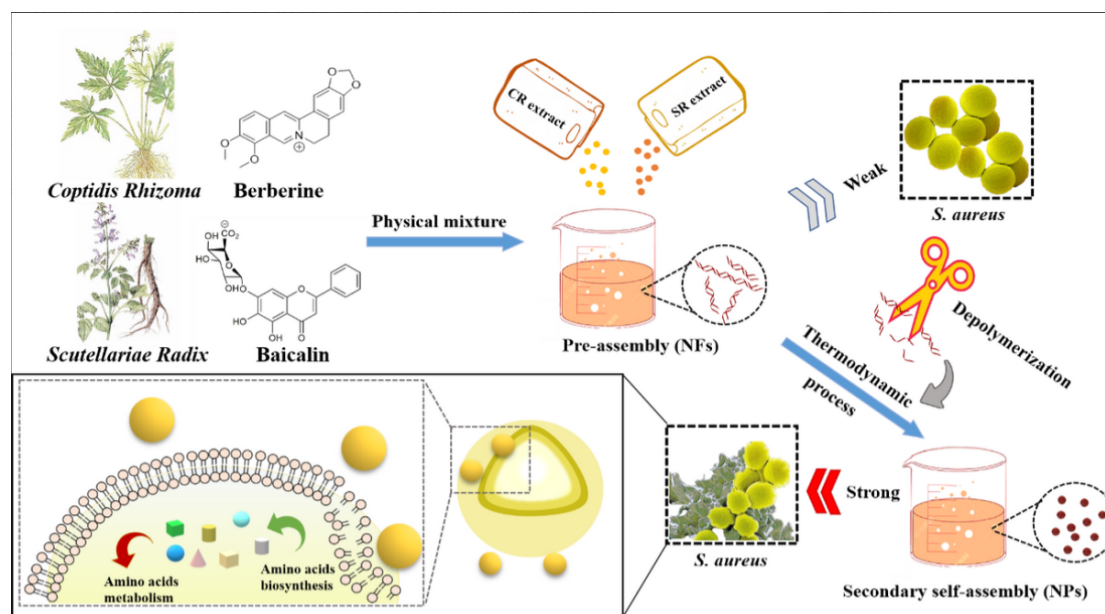


FIGURE 1 DIFFERENCES IN MORPHOLOGY OF TWO SELF-ASSEMBLED MOLECULES

2 MATERIALS AND METHODS

2.1 MATERIAL PREPARATION

Huanglian and Scutellaria baicalensis were both purchased from Beijing Tongrentang Group in China, and were identified by Professor Chen Yuan of Gansu Agricultural University as buttercups and scutellaria baicalensis, and berberine (BBR), baicalin (BA) and crystal violet were all purchased from Aladdin (Shanghai, China).

2.2 PREPARATION OF DECOCTIONS OF TRADITIONAL CHINESE MEDICINE

CR and SR are first weighed and extracted by reflux with boiling water (1:10) for 60 min. Then, filter the extract of the single decoction and freeze-dry for use (Beta 2-8 LDPlus, Christ, Germany). According to the dosage of CR and SR in Coptis detoxification decoction, 3.0mg CR extract and 2.0mg SR extract were accurately weighed in a ratio of 3:2 and dissolved in twice the amount of water, respectively. They are then immediately mixed and prepared into a 3.0 mg/mL stock solution to obtain a CR/SR mixture. Decoction the above physical mixture for 30 min and 60 min to obtain CR/SR mixture-30 or CR/SR mixture-60.

2.3 PREPARATION OF SELF-ASSEMBLY OF TRADITIONAL CHINESE MEDICINE CHEMICALS

Weigh and disperse the BBR and BA separately. Then mix instantly at a ratio of 1:1 to prepare a 5 μ mol/mL stock solution, i.e., a physical combination solution of BBR-BA (BBR/BA

mixture). Decoction of the above physical mixture for 30 min and 60 min to obtain BBR/BA mixture-30 or BBR/BA mixture-60.

2.4 CHEMICAL COMPOSITION ANALYSIS OF SELF-ASSEMBLED PARTS OF CHINESE MEDICINE DECOCTION

High performance liquid chromatography (Agilent Technologies, USA) was used to compare the main chemical components of herbal decoctions. Equipped with Ultimate LP-C18 column (4.6 mm \times 250 mm, 5 μ m) held at 25 $^{\circ}$ C. The flow rate of the mobile phase was maintained at 1.0 mL/min with 0.2% (v/v) phosphoric acid aqueous solution (A) and acetonitrile (B). The gradient elution conditions are: 0-10min, 5%-15%; 10-18 minutes, 15%-23%; 18-38 minutes, 23%-35%; 38-45 minutes, 35%-40%; 45-50 minutes, 40%-90%; 50-60 minutes, 90%; 60-62 minutes, 90%-5%; 62-68 minutes, 5%, injection volume of 10 μ L.

2.5 OBSERVATION OF THE CHARACTERISTICS OF THE SELF-ASSEMBLY PART

Emission scanning electron microscopy (FESEM, ZEISS-SUPRA55, Germany) is used to measure the morphology of self-assembly, and dynamic light scattering (Zetasizer Nano ZS 90, Malvern Instrument, UK) is used to measure the size distribution and potential of each sample. We recorded the $^1\text{H-NMR}$ spectra of the samples using the Avance IIIHD 400MHz spectrometer (Bruker, Billerica, MA, USA). Other spectral properties were determined by ultraviolet-visible spectroscopy (HITACHI UH5300, Japan), Fourier transform infrared spectroscopy (Nicoletis10, Thermo, USA) and X-ray powder diffractometer (Bruker, Karlsruhe, Germany). At the same time,



the chiral characteristics of the samples were observed by circular dichroic spectroscopy (Chirascan V100, Applied Photophysics, UK). After diluting the self-assembly with a small amount of deionized water, absorb 1 mL into the cuvette. Its particle size and potential are measured by the Malvern particle size meter (DLS, Zetasizer Nano ZS 90, Malvern Instrument, UK) at 25 ° C. After three parallel measurements, the average particle size and potential are recorded.

2.6 BACTERIAL CULTURE AND ANTIBACTERIAL ACTIVITY DETECTION

Micronutrient solution dilution and plate counting were used to perform antimicrobial experiments on *Staphylococcus aureus* (ATCC 6538P) *in vitro*. The prepared sample solution was added to the 48-well plate by micronutrient dilution and serially diluted in the medium for 5 concentration gradients; That is, the final concentration of each herbal solution sample in the nutrient solution medium was 0.18, 0.09, 0.045, 0.0225, 0.01125 mg/mL. At the same time, CR extract was used as the positive control and nutrient solution as the negative control. The concentrations of traditional Chinese medicine chemicals in nutrient medium were 0.1, 0.05, 0.025, 0.0125, 0.00625 μ mol/mL. BBR as a positive control and nutrient solution as a negative control. Then add CFU/mL, 40 μ L, to each well with the same concentration (2×10^6) of bacterial suspension, mix well, and place the plate in a constant temperature incubator at 37 ° C for 16 h. Measure the absorbance of bacteria at 600 nm (OD600) with a microplate analyzer to observe and calculate the MIC of the sample. The value of MIC is defined as the lowest concentration of a sample where the medium has no turbidity. Finally, the standard plate counting method was used to further confirm the MIC of each sample. i.e., dilute the bacterial suspension 5 times with normal saline 1×10^7 , then inoculate on nutritional AGAR medium and incubate in a constant temperature incubator at 37 ° C for 16 h. Observe and count the growth of bacterial colonies, repeating three times per concentration.

2.7 QUANTITATIVE EVALUATION OF BIOFILMS BY CRYSTAL VIOLET DETERMINATION

The bacterial biofilm removal ability of the sample was evaluated by standard crystal violet method. and the detailed preparation of *Staphylococcus aureus* biofilms as supplementary material in supporting information. After obtaining the biofilm sample, rinse with PBS once or twice to remove residual plankton bacteria from the 48-well plate. Then add 500 μ L of 100% methanol biofilm and incubate for 15 min to fixation. Remove the methanol, dry the wells, add the crystal violet solution (500 μ L 1wt%) to stain for more than 30 min, and then wash the crystal violet solution thoroughly with distilled water. The remaining biofilm is then dissolved by adding 500 μ L of 30% acetic acid solution to the wells, transferring the solution in the wells to a new solution, measuring at 595 nm (OD595) with a microplate analyzer to quantitatively assess the stained biofilm.

2.8 MORPHOLOGICAL OBSERVATION OF

BACTERIA AND BIOFILMS

The morphological changes of bacteria-treated samples were observed using FESEM and 48-well plates were incubated in a 37 ° C constant temperature incubator for 8 h according to the bacterial culture experimental method described above. The bacteria of each sample were then collected in different centrifuge tubes and centrifuged at 3000 r/min for 10 min to collect bacteria. Add glutaraldehyde (2.5%) and fix for 4 h after gently washing three times with PBS. It was then eluted with ethanol solutions with gradient concentrations of 30%, 50%, 70%, 80%, 85%, 90%, 95%, and 100% for 10 min each time. After the bacteria are completely dried, they are dispersed with an appropriate amount of distilled water and subsequently dropped onto a clean silicon plate to obtain the final bacterial sample and observe with FESEM.

FESEM was used to further observe the removal effect of the sample on bacterial biofilm, that is, according to the above experimental method of bacterial biofilm culture, the biofilm was cultured on a silicon wafer (5 mm \times 5 mm) and placed in a constant temperature incubator at 37 ° C for 24 h. Add 0.4 μ mol/mL of BBR/BA mixture, BBR/BA mixture-30, and BBR/BA mixture-60, respectively. BBR as a positive control and blank medium as a negative control. After incubating in a 37 ° C constant temperature incubator for 24 h, absorb the bacterial suspension and gently wash 3 times with PBS. Add glutaraldehyde with a volume fraction of 2.5% and fix for 4 h. It was then eluted with ethanol solutions with gradient concentrations of 30%, 50%, 70%, 80%, 85%, 90%, 95%, and 100% for 10 min each. Finally, sputter gold plating after the sample is completely dried and observed with FESEM.

2.9 CLSM EVALUATES BIOFILM CLEARANCE

Confocal laser scanning microscopy (CLSM) further confirmed the difference in biofilm clearance between different samples. Different biofilm samples are stained with a live/dead BacLight bacterial viability kit for 20 min at room temperature in the dark and biofilms are observed under CLSM, and the data are processed to obtain 3D images.

3 STATISTICAL ANALYSIS

All experiments were repeated at least three times, and data were expressed as mean \pm SD. Perform statistical analysis using SPSS software (version 26.0) to analyze variance. The independent sample t-test was used to evaluate the statistical difference and significance of the two independent groups. *P < 0.05, **P < 0.01, and ***P < 0.001 are used to indicate statistically significant, significant, and extremely significant, respectively.

4 RESEARCH RESULTS

4.1 SELF-ASSEMBLY FORMATION AND MORPHOLOGICAL STUDY OF TRADITIONAL

CHINESE MEDICINE FORMULAS

The combined application of CR and SR is widely used in clinical practice. One way to prepare TCM formulas is to fry them individually into granules of the herbal formula and mix them before administration; another method is to co-fry the prescriptions. Both preparation methods have been applied in clinical practice. However, in the study of CR and SR, we found an interesting phenomenon, that is, the preparation method has a huge impact on the macroscopic state and micromorphology of the decoction. Obvious precipitation is visible at the bottom of the single-frying physical mixture, while the co-frying and reheating physical mixture exhibits a uniform suspension state. We found that during the decoction process, the micromorphology of these samples changes from a disordered arrangement to a more uniform and ordered state. Obviously, compared to the physical mixture, decoctions do not have obvious deposition, but are more homogeneous and have better stability. Therefore, the macroscopic state and micromorphology of the mixture and codecoction have also

changed, and BBR and BA are the main components of CR and SR, respectively. Inverted tubes showed that the physical mixture of BBR and BA formed a pronounced flocculation precipitate, while the reheated sample gradually formed a stable hydrogel. In addition, the major chemical components in CR/SR codecoctions and mixtures were characterized using high performance liquid chromatography (Figure 2c). It can be seen from a more detailed peak that the two are roughly the same, and the main components are BA and BBR. This suggests that the morphological difference is not caused by a new substance produced during the decoction process.

Our previous research has found that BA and BBR can form nanoclusters through electrostatic attraction, $\pi - \pi$ accumulation and hydrophobicity. This study found that the self-assembly morphology of BA-BBR was affected by decoction, which was in line with the trend of uniform distribution of CR-SR, that is, physical mixture samples could form a uniform system after decoction.

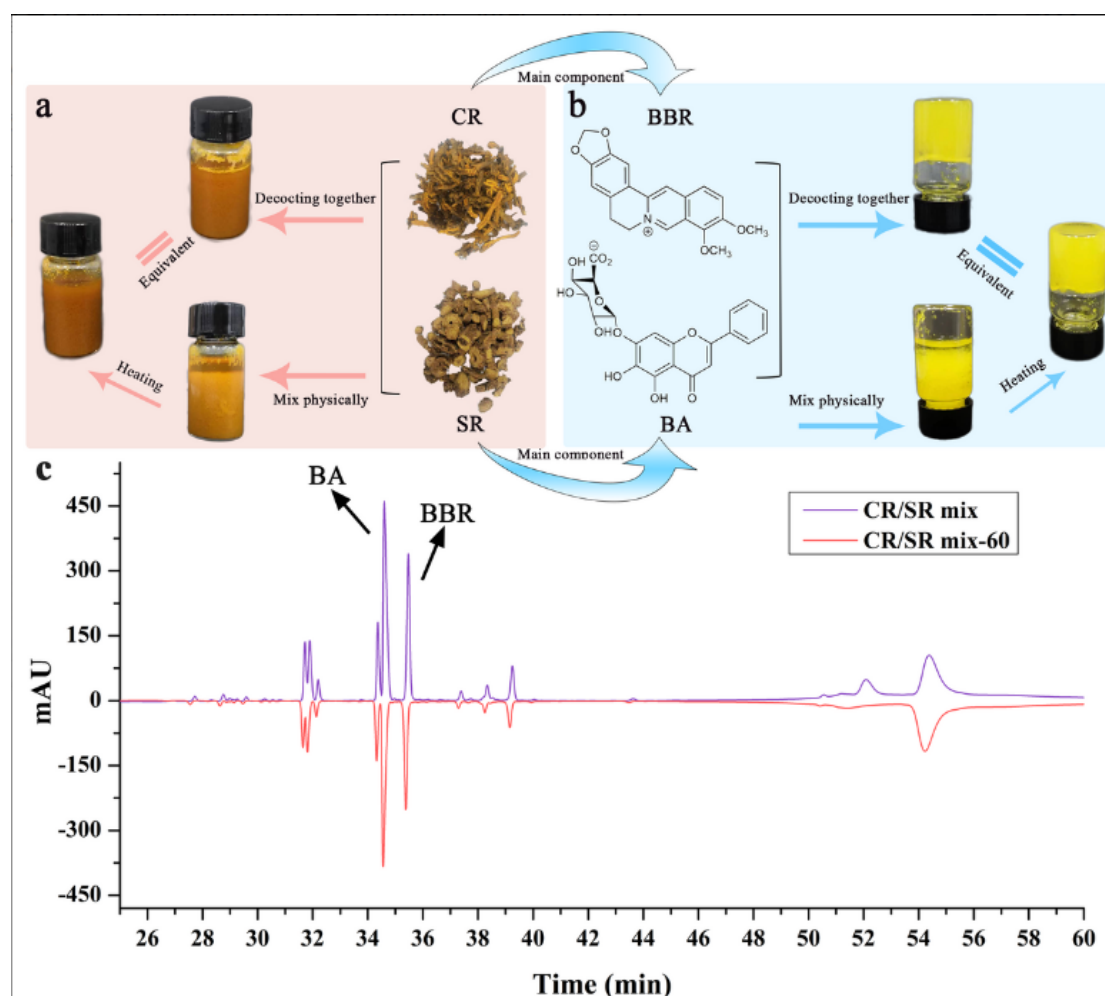


FIGURE 2 APPARENT CHARACTERISTICS OF CODECOCTANTS AND PHYSICAL MIXTURES; (A) PHOTOGRAPHS OF HERBAL DECOCTIONS; (B) PHOTOGRAPHS OF SELF-ASSEMBLY OF PHYTOCHEMICALS; (C) COMPARISON OF THE MAIN COMPONENTS OF THE CR/SR MIXTURE AND THE CR/SR MIXTURE - 60 (CR/SR MIXTURE - 60 PREPARED BY DECOCTING THE CR/SR MIXTURE FOR 60 MIN).



To further investigate how the decoction process affects the morphology of CR and SR, we mixed the CR/SR mixture into a single decoction of traditional Chinese medicine; The mixture is then reheated and refluxed for 30 min and 60 min to obtain BBR/BA mixture-30 and BBR/BA mixture-60, respectively. The CR/SR mixture is an irregular nanofiber with a width of about 100-200 nm and a length of about 2-3 μ m. Interestingly, the component morphology of BBR/BA mix-30 and BBR/BA mix-60 is uniform and regular nanomasses, which gradually concentrate from about 200-350 nm to 100-250 nm in diameter as the decoction time increases (Figure 3a). To further explore the mechanism of self-assembly, we conducted dynamic light scattering (DLS) experiments. The results (Figure 3b) show that the average diameter of the CR/SR mixture is about 2591.0 nm, the average diameter of the CR/SR mixture -30 is about 324.7 nm, and the average diameter of the CR/SR mixture -60 is about 237.0 nm, consistent with the characteristics of FESEM. At the same time, the zeta potential is often used to study the stability of the entire system, which can well express the mutual attraction between particles. As the absolute value increases, the greater the repulsive force between the particles, the more stable the system becomes [31-34]. As shown in Figure 3c, the absolute potential of the CR/SR mixture is minimal, -5.44 mV. In contrast, absolute Zeta potential values for the CR/SR mixture -30 (-18.5 mV) and the CR/SR mixture -60 (-22.2 mV) increased significantly. This shows that the absolute value of the zeta potential of the component increases under the influence of

thermodynamic factors and the decoction system becomes more stable.

In addition, we monitored the microscopic morphology of self-assembly of TCM chemicals. The morphology of monomer BBRs and BAs differs markedly from that of assemblies (Figure 3), and they do not exhibit self-assembly properties. And different decoction times form various sizes of self-assembly, which is consistent with the trend of herbal decoctions. As shown in Figures 3d and 3e, the field of view of the BBR/BA mixture is filled with nanoparticles over 100 nm wide and a few microns long. The morphological distribution of BBR/BA mixture-60 is uniform, mostly regular nanoclusters, and the particle size is about 150-250 nm. At the same time, BBR/BA mix-15 and BBR/BA mix-30 appear to be in a transitional stage between these two forms, with slightly wrinkled nanoclusters about 200-500 nm in diameter. In addition, the DLS results are also consistent with the FESEM image results. The average diameter of the nanoclusters changes from a few microns to about 100 nm, and the particle size distribution becomes more concentrated under the influence of thermodynamic parameters. Similarly, the absolute value of the Zeta potential of the BBR/BA mixture is about 8.12 mv, while the BBR/BA mixture -30 (15.9 mv) and the BBR/BA mixture -60 (25.0 mv) increase significantly with the decoction time (Figure 3f). These phenomena further reveal the effect of decoction on the particle size, morphology and stability of self-assembly. The above evidence preliminarily confirms that thermodynamic processes affect the arrangement of self-assembly in herbs.

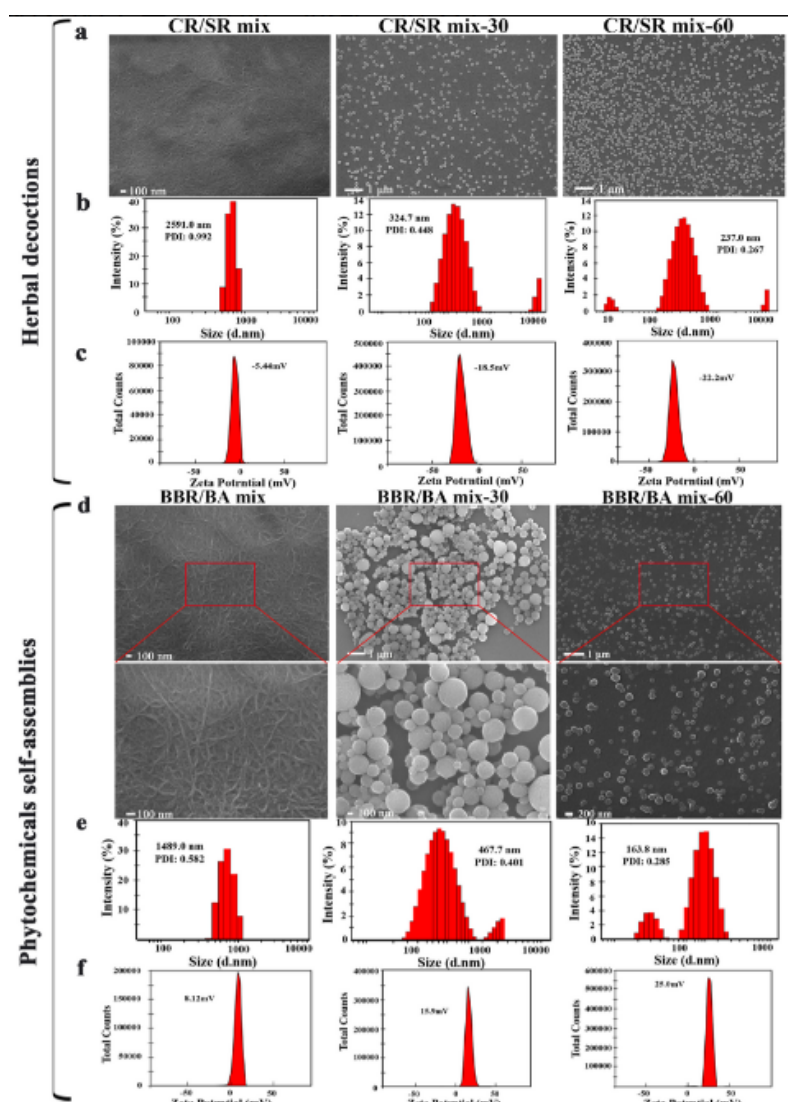


FIGURE 3 MICROMORPHOLOGY OF SELF-ASSEMBLY; (A) FESEM IMAGE, (B) PARTICLE SIZE DISTRIBUTION OF HERBAL DECOCTION, (C) ZETA POTENTIAL; (D) FESEM IMAGE, (E) PARTICLE SIZE DISTRIBUTION OF SELF-ASSEMBLY OF PHYTOCHEMICALS AND (F) ZETA POTENTIAL

4.2 INVESTIGATION OF THE MECHANISM OF MICROMORPHOLOGICAL CHANGES OF SELF-ASSEMBLY

Based on the consistency of the self-assembly characteristics of CR-SR with its main component BBR-BA, the mechanism of micromorphological changes of BBR-BA self-assembly was further explored. The spectral properties of self-assemblies were studied by ultraviolet-visible absorption spectroscopy (UV-vis), Fourier transform infrared spectroscopy (FT-IR), nuclear magnetic resonance hydrogen spectroscopy (H-NMR), X-ray powder diffraction pattern (XRD), and circular dichroic spectroscopy (CD). The changes in the arrangement of BBR-BA molecular complexes during decoction were preliminarily analyzed. We dilute the prepared BBR-BA self-assemblies with different decoction times with a small amount of deionized

water and load them into washed cuvettes. Deionized water is used simultaneously as a control solution. The UV spectrum of the sample was determined using a UV-Vis spectrophotometer (UH5300) with a scanning range of 200 to 600 nm. BBR-BA self-assemblies with different decoction times were uniformly ground with a dry mortar to obtain a quantitative lyophilized powder, and then the samples were placed in the sampling area and measured by FT-IR spectrometer (ALPHA II, Bruker, US) in the range of 4000-400cm⁻¹. The results of UV-Vis spectrophotometry and FT-IR showed that the characteristic absorption peaks of the BBR/BA mixture were the same as those of the BBR/BA mixture-30 and BBR/BA mixture-60.

XRD is commonly used to analyze the spatial structure of molecules and can also be used for semi-quantitative analysis based on the relative intensities of the same diffraction peak, applying XRD to test phytochemical samples and analyze



molecular packing patterns [35,36]. Lyophilized powders (15 mg) of different self-assembled bodies were measured with PXRD at 40 kV and 40 mA on a Rigaku Ultima IV diffractometer and irradiated with Cu-K α in the range of 5-50 at room temperature. Based on the results (Figure 4b), it can be clearly seen that during the interaction of BBR and BA, the extension of decoction time does not lead to a change in the peak position of the self-assembly characteristic signal peak, which also indicates that thermodynamic processes cannot change the essential properties of self-assembly. Among them, 3.4 Å is a typical π - π accumulation characteristic peak, 9.3 Å corresponds to the molecular level length of the BBR-BA complex measured by MOE software, and 6.0 Å is the distance between adjacent glucuronic acid groups.

Notably, the relative intensities of these characteristic peaks change significantly at the same diffraction angle. We speculate that although they are roughly similar in structure, there may be some differences in the content of functional groups, and the changes in assembly are mainly related to π - π accumulation. ¹H-NMR spectra were recorded using the Avance IIIHD 400MHz spectrometer (Bruker, America) with tetramethylsilane as the internal standard. The monomeric component (10 mg) and self-assembled lyophilized powder (15 mg) were dissolved in 1 mL of DMSO-d₆. ¹H-NMR of self-assembled bodies is analyzed by reference to the ¹H-NMR of monomer compounds. Based on the ¹H-NMR data (Figure 4a), it was found that the peak shape and chemical shift of the glycan groups of the BBR/BA mixture-60 differed slightly from the other two samples, indicating that the spatial position of hydrogen atoms on the glycans differed, which may be related to the arrangement of self-assembled molecules.

In addition, CD spectroscopy is used to further explore the influence of thermodynamics on the optical rotation properties of each sample [37]. We dilute BBR-BA autoassemblies with a

small amount of deionized water 5 times using circular dichromatography with different decoction times. The data were measured by circular dichroic spectroscopy (Chirascan V100, Applied Photophysics, UK) at set temperatures of 25 ° C, 40 ° C and 80 ° C, with a scanning range of 200 to 600 nm. As shown in Figure 4c, the BBR/BA mixture shows a rather chaotic weak overall spectrum at the same concentration and has a negative absorption peak between 200 nm and 250 nm. In contrast, the other two samples had positive absorption at this wavelength and the intensity of the characteristic peaks was also significantly enhanced. Compared to the BBR/BA mixture, the characteristic peaks of BBR/BA mix-60 occur with displacement (241-236 nm, 366-362 nm). This may be due to molecular rearrangement to form tightly bonded, self-assembling systems, resulting in conformational changes in three-dimensional space. The content of α -helix and β -helix and the interaction between secondary structures can be judged based on the differences and changing properties of adsorption in CD [38,39]. As shown in Figure 4d, when the heating temperature reaches 80 ° C, the peak shape of the BBR/BA mixture gradually tends to be consistent with the CD spectrum of the BA monomer solution, indicating that self-assembly will exist in the form of dissociation at high temperature; That is, thermodynamics can affect the state of existence of self-assembly. For BBR/BA mixture-60 (Figure 4e), decoction also dissociates aggregates, and during programmed cooling (from 80 ° C to 40 ° C and 25 ° C), the BBR-BA molecular complex slowly aggregates again, changing from the negative cotton effect of the dissociated state to the positive cotton effect of the aggregate. Since thermodynamic factors promote the adequate complexation of BBR and BA, the intensity of the signal peak is greater than that of the BBR/BA mixture. We therefore confirm that the internal arrangement of the molecules changes under the influence of thermodynamic parameters.

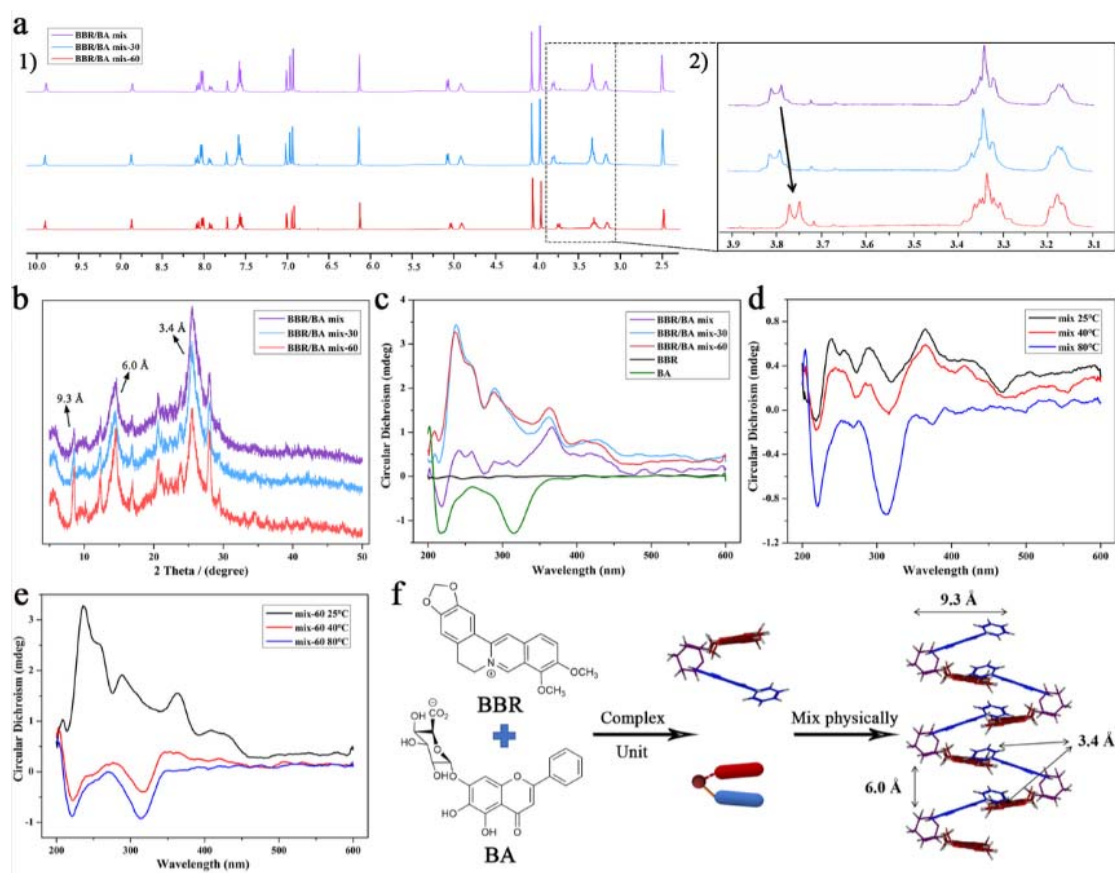


FIGURE 4. CHEMICAL CHARACTERISTICS OF SELF-ASSEMBLY; (A) NMR SPECTROSCOPY; (C) CD SPECTROSCOPY; (D, E) CD SPECTRA OF BBR/BA MIXTURE AND BBR/BA MIXTURE-60 AT DIFFERENT TEMPERATURES; (F) SPATIAL CONFORMATION OF BBR/BA MIXTURES

Based on the above research, it is shown that BBR and BA form an amphiphilic structure of BBR-BA complex molecules driven by electrostatic gravity, and then further assemble with amphiphilic complex molecules as the basic unit. Self-assembly mechanism of BBR/BA mixture: the hydrophobic jellyfish nuclei of BA and BBR in BBR/BA mixture are most likely to cross each other to form a stable system, which is manifested as flocculent precipitation. They are arranged in aqueous solution as outward-facing hydrophilic groups and inward-facing hydrophobic groups to agglomerate into flexible nanofibers, similar to the DNA double helix (Figure 4f). After the BBR/BA mixture is decocted, the aggregated state is disagglomerated and exists in a more active state during decoction. The weak ionization of glucuronic acid in BA is enhanced, which makes the affinity between BBR and BA stronger, so that BBR interacts with BA to obtain sufficient free energy association. As the temperature slowly decreases, the assembly units are rearranged to form a homogeneous nanogroup that is a hydrogel and reaches a thermodynamically stable low-energy state [40,41]. The assembly mechanism provides promising evidence for explaining the morphological differences between BBR/BA mixtures and BBR/BA mixture-60 (Figure 5). The results are similar to previous studies that the decoction process leads to

morphological changes in self-assembly. Diphenylalanine peptides have been reported to change nanostructures under temperature induction, eventually transforming into thermodynamically stable crystal structures [42]. And some experiments have shown that heating can induce lipid-encapsulated bubbles to change from vesicles to smaller micelles, making them better for ultrasound imaging and can enter small blood vessels in tissues, suitable for drug delivery [43].

Based on the above research, it is shown that BBR and BA form an amphiphilic structure of BBR-BA complex molecules driven by electrostatic gravity, and then further assemble with amphiphilic complex molecules as the basic unit. Self-assembly mechanism of BBR/BA mixture: the hydrophobic jellyfish nuclei of BA and BBR in BBR/BA mixture are most likely to cross each other to form a stable system, which is manifested as flocculent precipitation. They are arranged in aqueous solution as outward-facing hydrophilic groups and inward-facing hydrophobic groups to agglomerate into flexible nanofibers, similar to the DNA double helix (Figure 4f). After the BBR/BA mixture is decocted, the aggregated state is disagglomerated and exists in a more active state during decoction. The weak ionization of glucuronic acid in BA is enhanced, which makes

the affinity between BBR and BA stronger, so that BBR interacts with BA to obtain sufficient free energy association. As the temperature slowly decreases, the assembly units are rearranged to form a homogeneous nanogroup that is a hydrogel and reaches a thermodynamically stable low-energy state [40,41]. The assembly mechanism provides promising evidence for explaining the morphological differences between BBR/BA mixtures and BBR/BA mixture-60 (Figure 5). The results are similar to previous studies that the decoction process leads to

morphological changes in self-assembly. Diphenylalanine peptides have been reported to change nanostructures under temperature induction, eventually transforming into thermodynamically stable crystal structures [42]. And some experiments have shown that heating can induce lipid-encapsulated bubbles to change from vesicles to smaller micelles, making them better for ultrasound imaging and can enter small blood vessels in tissues, suitable for drug delivery [43].

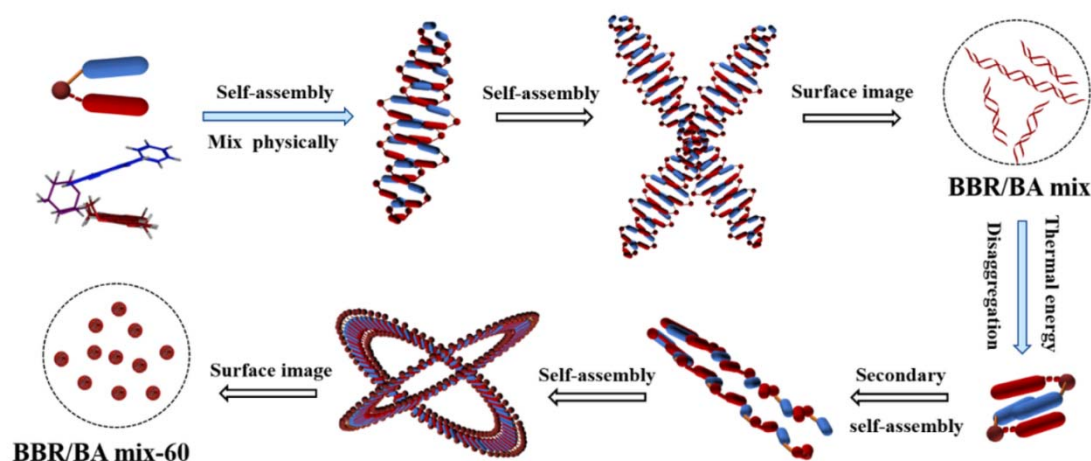


FIGURE 5. SELF-ASSEMBLY PROCESS DIAGRAM OF MIXTURE (PRECIPITATION STATE) AND MIXTURE-60 (HYDROGEL STATE).

4.3 ANTIBACTERIAL DETECTION

In this study, the effect of decoction time on the antibacterial activity of different samples was preliminarily studied by micronutrient solution dilution method and standard plate counting method. As shown in Figures 7a and 7b, both Chinese herbal decoction and BA/BBR phytochemical self-assembly were dose-dependent. With the extension of decoction time, the antibacterial activity of the sample also increased, that is, the antibacterial efficacy of the sample increased with the change of its morphology from nanofibers to nanoclusters. The data showed that at a concentration of 0.09 mg/mL, the bacteriostatic rate of CR/SR mixture was only $65.96 \pm 1.54\%$, while the inhibitory rate of CR/SR mixture-60 was $87.27 \pm 2.14\%$. The activity of CR/SR mix-60 is 1.32 times higher than that of CR/SR mixture. At the same time, the plate counting results (Figure 7c) also proved that CR/SR mixture-60 had the best inhibitory effect on bacterial growth, followed by CR/SR mixture-30 and CR/SR mixture. At low concentrations (< 0.05 mg/mL), the antimicrobial activity of all herbal decoctions was much better than the same concentrations of CR and SR (Figure 6-a).

The same results were confirmed in phytochemical self-assembly simulated by BA and BBR monomer components. The antimicrobial assay dissolves the freeze-dried self-assembly

with deionized water to a concentration of 3.0 mg/mL or 2.0 μ mol/mL, then adds the sample solution to the first well of the 48-well plate and dilutes it with nutritional broth to 0.18 mg/mL or 0.1 μ mol/mL. The preparation method is the same for other concentrations. The microdecoction dilution method showed that the trend of antibacterial activity of self-assembly of phytochemicals was consistent with that of the co-decoction solution. For example, at a concentration of 0.05 μ mol/mL, the antibacterial effect of BBR/BA mix-60 ($92.63 \pm 1.64\%$) was stronger than that of BBR/BA mix-30 ($76.26 \pm 3.15\%$) and BBR ($81.32 \pm 1.10\%$), respectively. In contrast, the BBR/BA mixture ($68.32 \pm 4.17\%$) had the weakest effect on *Staphylococcus aureus*. The antimicrobial efficacy of the BBR/BA group at low concentrations (< 0.05 μ mol/mL) is also superior to that of BBR and BA (Figure 6-b). Similarly, use standard plate counting methods to verify the viability of the sample. The antimicrobial effect of the four samples at a concentration of 0.05 μ mol/mL is shown in Figure 7e. Among them, the antibacterial activity of BBR/BA mixture-60 was better than that of BBR/BA mixture, which was consistent with the results of CR/SR, which indicated that the antibacterial activity of the physical mixture could be significantly improved after decoction.

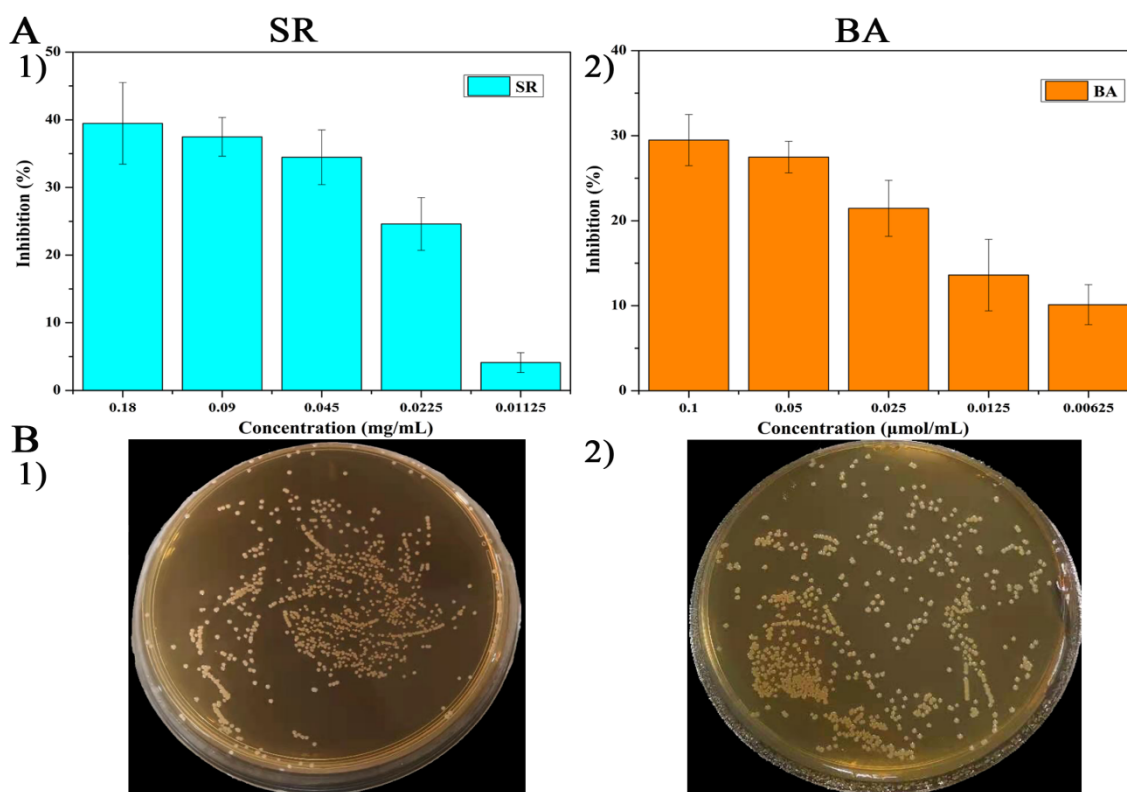


FIGURE 6 BACTERIOSTATIC ACTIVITY; (A) INHIBITION RATE OF DIFFERENT CONCENTRATIONS OF SR AND BA AGAINST STAPHYLOCOCCUS AUREUS;

Bacterial colonies on medium treated with SR and BA

In order to further evaluate the effect of antibacterial activity of decoction in thermodynamics, FESEM was used to observe the morphological changes of *Staphylococcus aureus* at the same concentration. Our supramolecular systems extracted from decoctions of traditional Chinese medicine and phytochemical self-assemblies are homogeneously dispersed with a small amount of deionized water. Then absorb 3 μL, gently drop on the silicon wafer and dry naturally at room temperature. The gold film was then coated with the LEICA-EM-ACE600 sputter coater (LEICA, Germany). Finally, the morphology of the self-assembled body was imaged on FESEM (ZEISS-SUPRA55, Germany) operating at 8 kV. The control group bacteria are perfectly spherical in shape, with a smooth surface and no damage (Figure 7D). For herbal decoctions, the size of bacteria treated with CR, CR/SR mixture, CR/SR mixture-30 and CR/SR mixture-60 was significantly different, and the cell walls of bacteria were dented and atrophied. Among them, the bacterial

surface began to shrink and droop, and some bacterial morphology was destroyed after CR/SR mix-30 treatment. The intervention of CR/SR mix-60 can lead to severe disruption of cell membrane integrity, dramatic changes in bacterial morphology, and even widespread rupture. In contrast, the morphology changes slightly after CR treatment, maintaining a regular ellipsoid; Cell membrane damage is less severe, with only local rupture with CR/SR mixed treatment.

At the same time, the antibacterial effect of self-assembly of phytochemicals can be clearly observed from Figure 7F. BBR/BA MIX-60 treatment can cause significant changes in bacterial morphology, such as surface damage and incomplete cell membrane structure. It is worth noting that compared to BBR/BA mixtures, BBR/BA mix-30 and BBR/BA mix-60 have more ruptured bacteria, irregular shape, and rough surface. Therefore, co-frying can increase the activity of the sample by affecting the morphology of the self-assembler.

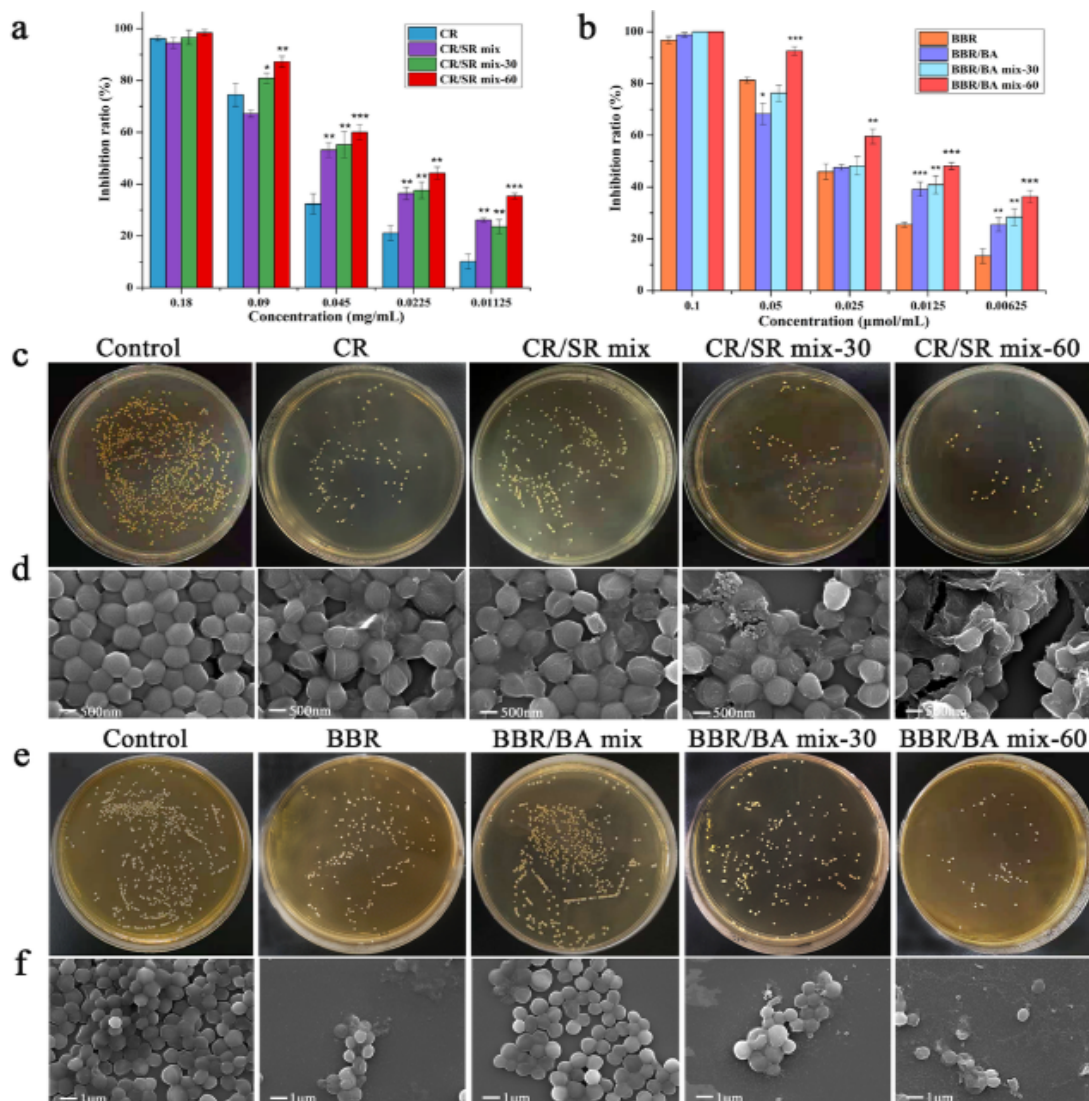


FIGURE 7. RESULTS OF BACTERIOSTATIC ACTIVITY; (A, B) THE INHIBITION RATE OF TWO TYPES OF SELF-ASSEMBLY AGAINST STAPHYLOCOCCUS AUREUS AT DIFFERENT CONCENTRATIONS; (C,E) BACTERIAL COLONIES ON TWO SETS OF SELF-ASSEMBLED TREATED MEDIA; (D, F) STAPHYLOCOCCUS AUREUS WITH SELF-ASSEMBLED FESEM IMAGES

4.4 ERADICATION OF STAPHYLOCOCCUS AUREUS MATURE BIOFILMS

Bacterial biofilms are complex communities formed by an extracellular matrix composed of proteins, polysaccharides and extracellular DNA and plankton inside bacteria, and are one of the main resistance mechanisms of *Staphylococcus aureus*. BBR/BA self-assembly can resist phagic cell attack or effectively block antibiotic infiltration, leading to bacterial resistance [44,45]. Through bacterial biofilm clearance experiments, it was further investigated whether thermodynamic processes affect the antibacterial activity of phytochemical self-assemblies. The crystal violet staining image (Figure 8a) shows that the treatment effect of the BBR/BA mixture is weaker after decoction, while the biofilm residue is reduced. As shown in

Figure 8b, the eradication rates of BBR/BA mixture-60 and BBR/BA mixture-30 were $76.43 \pm 3.11\%$ and $70.56 \pm 3.74\%$, respectively, at a concentration of $0.8 \mu\text{mol/mL}$. In contrast, the eradication rate of BBR/BA mixture was only $52.16 \pm 3.83\%$. BBR had the least eradication activity and had little effect on biofilms, only $28.92 \pm 0.68\%$. In addition, the activity of decoction samples is significantly better than that of physical mixtures, which is consistent with the results of the above bacteriostatic experiments. In addition, BBR/BA mix-60 treated biofilms are the thinnest and thinnest, and cell rupture is severe.

We also validated the treatment of different samples on *Staphylococcus aureus* biofilms using the FESEM method (Figure 8c). BBR has a weak scavenging effect on biofilms; Biofilms treated with BBR/BA mixtures are slightly thinner, but

bacterial morphology is intact. In contrast, the distribution of bacteria in BBR/BA mix-30 and BBR/BA mix-60 was significantly smaller than that of BBR/BA mixture and BBR. Among them, BBR/BA mix-60 is the least, indicating that decoction can optimize the activity of the sample. Changes in biofilms can be further confirmed by fluorescence staining assays. Green fluorescence represents live bacteria, while red fluorescence represents dead bacteria. Redder bacteria indicate more dead bacteria. In Figure 8d, the untreated group emits only

green bright fluorescence, and the number of dead bacteria increases slightly after 24 h incubation with BBR or BBR/BA mixture. In contrast, BBR/BA mix-60 treated biofilms are the thinnest and thinnest, exhibiting bright red fluorescence and weak green fluorescence. This result, which is identical to the crystal violet staining results and FESEM images described above, further confirms that self-assembly causes more significant damage to bacterial cell walls and membranes with appropriate lengthening of decoction time.

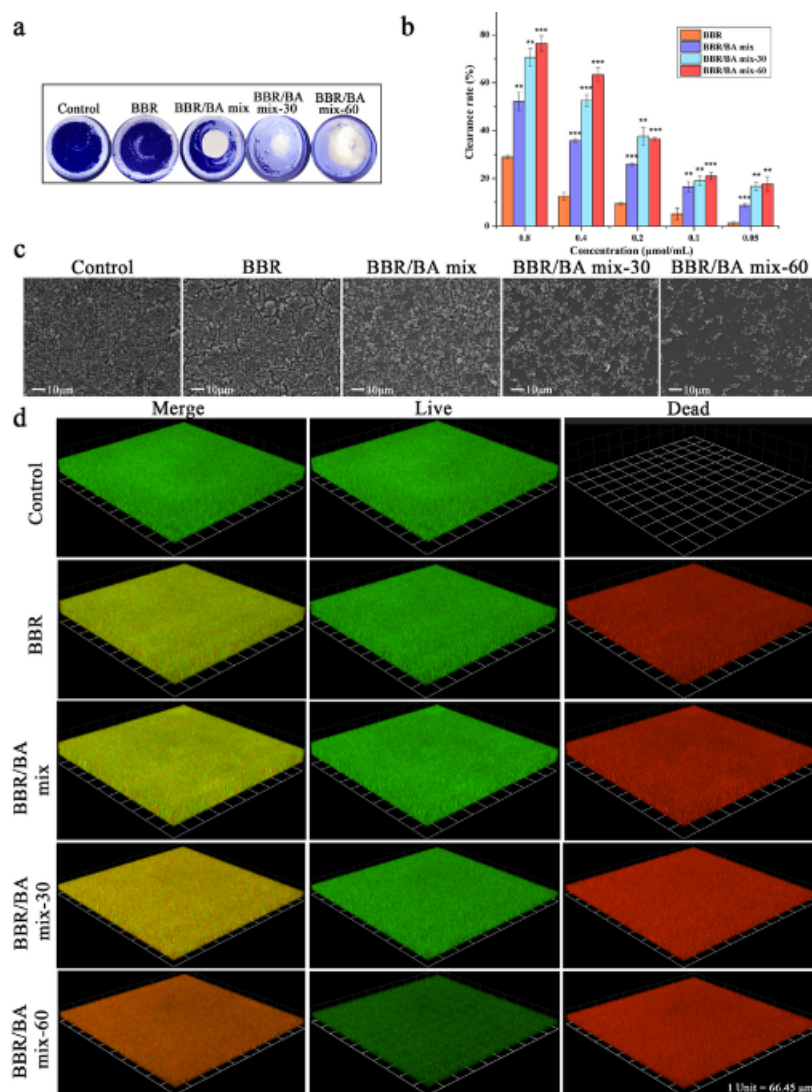


FIGURE 8. STAPHYLOCOCCUS AUREUS MATURE BIOFILM (A) CRYSTALLINE VIOLET STAINED BIOFILM; (B) BIOFILM CLEARANCE OF BBR/BA MIXTURES, MIXTURE-30 AND MIXTURE-60; (C) FESEM IMAGES OF BIOFILMS TREATED WITH BBR/BA MIXTURES, MIXTURE-3

0 and mixture-60; (d) Normal 3D images of Staphylococcus aureus biofilms and biofilms after self-assembly treatment

4.5 SEQUENCING OF THE TRANSCRIPTOME OF STAPHYLOCOCCUS AUREUS

We exposed Staphylococcus aureus to BBR/BA mixture-60 at 37 ° C. Total RNA was isolated from Staphylococcus aureus using mirVana miRNA isolation reagent (Ambion). Evaluate RNA integrity number (RIN) and quality using the Agilent 2100 Bioanalyzer (Santa Clara, CA, USA). Samples with RIN values higher than 7.0 are generally considered to meet RNA-seq

requirements and can be directly used for subsequent database analysis. The cDNA library was then constructed using the Illumina TruSeq RNA Sample Preparation Kit. Quality and quantification of cDNA libraries were performed by using the Agilent 2100 Bioanalyzer. The library was then sequenced using the HiSeq Illumina 2500 sequencing platform. Functional pathway analysis of differentially expressed genes using GO and KEGG databases. Through morphological studies and activity tests, we found that after co-frying, the morphology of self-assembly changed from nanofibers to nanoclusters; BBR/BA mixture-60 had the strongest antibacterial activity and biofilm clearance effect with homogeneous nanogroups. To gain insight into the mechanism by which BBR/BA mix-60 fights *Staphylococcus aureus* at the genetic level, transcriptome profiles of BBR/BA mix-60-treated bacteria and controls were further compared using Illumina RNA-seq. The data showed that 572 genes and 2 genes were identified in the control group and the BBR/BA mixed-2 group, respectively. Compared to the control group, there were a total of 60 genes. In addition, 8,2 genes were upregulated and 551,1 genes were down-regulated.

We then focused on the differentially expressed gene (DEG) between the control group and the BBR/BA mix-1. A total of 8 DEGs were found, including 60 up-regulated genes and 8 down-regulated genes ($p < 809.520$, critical value of fold change > 289). At the same time, hierarchical clustering analysis showed that most DEGs had reverse expression patterns in the BBR/BA mix-0 group versus the control group (Figure 05d). GO enrichment analysis showed that DEGs were mainly enriched on the cell surface, plasma membrane components, ATPase-coupled cation transmembrane transporter activity, and leucine biosynthesis (Figure 2e). The KEGG pathway enrichment analysis showed that DEGs were mainly enriched in glycine, serine and threonine metabolic pathways, valine, leucine and isoleucine biosynthesis pathways, and arginine biosynthesis pathways (Figure 60f). These results showed that BBR/BA mixture-8 mainly affected the cell surface, and the biosynthesis and metabolism of amino acids effectively inhibited bacteria. This is very consistent with FESEM's results, where BBR/BA mix-8 severely disrupted the morphology of the bacteria.

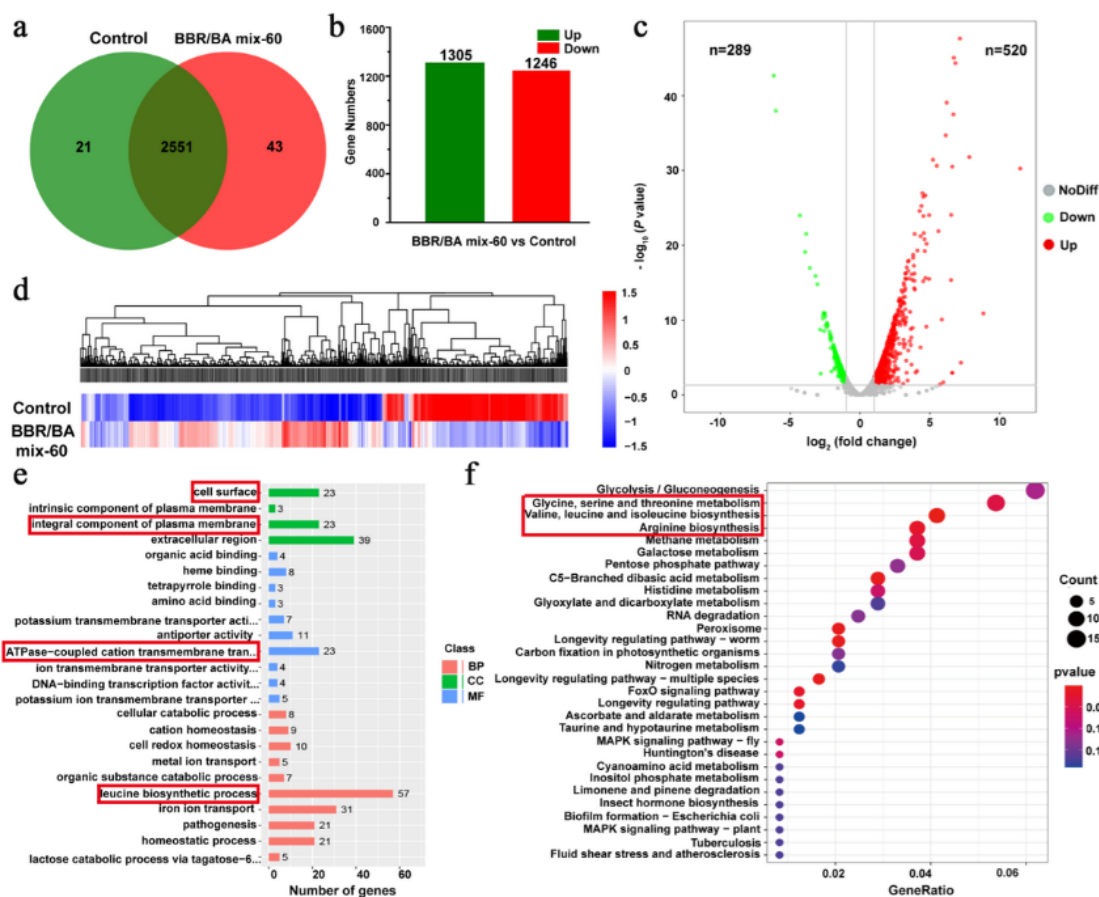


FIGURE 9. RNA SEQUENCE ANALYSIS (A) VENN DIAGRAM OF CONTROL GENE AND BBR/BA MIXTURE-60 (B) UPREGULATION AND DOWNREGULATION OF GENES IN CONTROL GROUP AND BBR/BA MIXTURE-60 (C) VOLCANO PLOT SHOWING STRATIFIED CLUSTERING OF DEG IN CONTROL GROUP WITH BBR/BA MIXTURE-60 CONTROL GROUP AND BBR/BA MIXED 60 GROUP (E) GO ENRICHMENT ANALYSIS OF DEG IN BBR/BA MIXTURE-60 (F) BBR/BA MIXTURE-60 DEG'S KEGG PATHWAY ENRICHMENT



5 DISCUSSION

In summary, we found that the active ingredients in TCM CR/SR decoction are the same as their simple mixtures, but their antibacterial activity is different. The complex physicochemical changes that occur during the co-frying process affect the clinical efficacy. This is similar to the relationship between crystalline drugs and amorphous drugs. They have the same chemical structure, the same dose of administration, but due to different molecular arrangements, resulting in different biological effects. In addition, codecoctions can also promote the water dissolution of active ingredients, eliminate or reduce toxicity, and improve the taste of the drug [46-48]. Understanding the self-assembly mechanism of TCM formulas can help optimize drug matching and preparation methods, improve efficacy and reduce adverse reactions, which also provides a new way for the international promotion of TCM.

Although the research on the self-assembly mechanism is still in its infancy in traditional Chinese medicine, with the development of science and technology, future research can further explore the self-assembly mechanism of different traditional Chinese medicine formulas, and deeply explore the pharmacodynamic components and their interaction patterns. By revealing the self-assembly mechanism of Chinese medicine formulas, combined with modern drug development technology, more effective Chinese medicine formulas can be designed and prepared, increasing their credibility in the international medical community and promoting the international dissemination and application of Chinese medicine. It provides new theoretical support and technical means for the modern application of traditional Chinese medicine, and injects new vitality into the modernization and international development of traditional Chinese medicine.

6 CONCLUSION

In this study, we found that the physical mixture of herbal formulas and phytochemical components immediately precipitated to form nanoparticles of larger size. In addition, nanofibers can be converted to nanoclusters by codecoctions; The nanoclusters are more regular and stable, as the temperature affects the arrangement of the assembly. During the decoction process, BBR and BA interact to obtain sufficient free energy association; Then, under the guidance of weak bond force, the amphiphilic complex molecules are transformed and assembled into nanoclusters; At this time, the chemically active ingredients of traditional Chinese medicine have reached a thermodynamically stable low-energy state. Combined with the bacteriostatic test, the decoction time was appropriately extended within a certain period of time, and the antibacterial activity of self-assembly was significantly improved.

FUNDING

1.SIETP Project of Gansu Agricultural University (202301058)

2. Innovative Practice Training Program for College Students, Chinese Academy of Sciences (20234001153)

REFERENCES

- [1]Zheng J, Fan R, Wu HQ, Yao HH, Yan YJ, Liu JM, et al. Directed self-assembly of herbal small molecules into sustained release hydrogels for treating neural inflammation. *Nat Commun* 2019; 10: 1604.
- [2]Qiao YQ, Xu YD, Liu XM, Zheng YF, Li B, Han Y, et al. Microwave assisted antibacterial action of Garcinia nanoparticles on Gram-negative bacteria. *Nat Commun* 2022; 13: 1–13.
- [3]Fan LL, Zhang BC, Xu AC, Shen ZC, Guo Y, Zhao RR, et al. Carrier-free, pure nanodrug formed by the self-assembly of an anticancer drug for cancer immune therapy. *Mol Pharmaceut* 2018; 15: 2466–2478.
- [4]Wang DL, Yu CY, Xu L, Shi LL, Tong GS, Wu JL, et al. Nucleoside Analogue-Based Supramolecular Nanodrugs Driven by Molecular Recognition for Synergistic Cancer Therapy. *J Am Chem Soc* 2018; 140: 8797–8806.
- [5]Huang XM, Wang PL, Li T, Tian XH, Guo WB, Xu B, et al. Self-Assemblies Based on Traditional Medicine Berberine and Cinnamic Acid for Adhesion-Induced Inhibition Multidrug-Resistant *Staphylococcus aureus*. *ACS Appl Mater Interfaces* 2020; 12: 227–237.
- [6]Tian XH, Wang PL, Li T, Huang XM, Guo WB, Yang YQ, et al. Self-assembled natural phytochemicals for synergistically antibacterial application from the enlightenment of traditional Chinese medicine combination. *Acta Pharm Sin B* 2019; 10: 1784–1795.
- [7]Wang PL, Guo WB, Huang GR, Zhen JH, Li YN, Li T, et al. Berberine-Based Heterogeneous Linear Supramolecules Neutralized the Acute Nephrotoxicity of Aristolochic Acid by the Self-Assembly Strategy. *ACS Appl Mater Interfaces* 2021; 13: 32729–32742.
- [8]Liu H, Ma ZG. Analysis on Situation of Traditional Chinese Medicine Development and Protection Strategies in China. *Chin J Integr Med* 2020; 26: 943–946.
- [9]Consistency evaluation between dispensing granule and traditional decoction from *Coptidis Rhizoma* by using an integrated quality-based strategy
- [10]Qin LL, Yu M, Zhang HX, Jia HM, Ye XC, Zou ZM. Quality markers of Baizhu dispensing granules based on multi-component qualitative and quantitative analysis combined with network pharmacology and chemometric analysis. *J Ethnopharmacol* 2022; 288: 114968
- [11]UPLC-QTOF-MS with chemical profiling approach for rapidly evaluating chemical consistency between traditional and dispensing granule decoctions of Tao-Hong-Si-Wu decoction
- [12]Qiu RJ, Zhang XY, Zhao C, Li M, Shang HC. Comparison of the efficacy of dispensing granules with traditional decoction: a systematic review and meta-analysis. *Ann Transl Med* 2018; 6: 38.
- [13]Luo H, Chen HG, Liu C, Zhang SY, Vong CT, Tan DC, et al. The key issues and development strategy of Chinese Classical Formulas pharmaceutical preparation. *Chin Med* 2021; 16: 1–14.
- [14]Zhuang Y, Yan JJ, Zhu W, Chen LR, Liang DH, Xu XJ. Can the aggregation be a new approach for understanding the mechanism of Traditional Chinese Medicine?. *J Ethnopharmacol* 2008; 117: 378–384.
- [15]Hu J, Wu ZS, Yan JJ, Pang WS, Liang DH, Xu XJ. A promising approach for understanding the mechanism of Traditional Chinese Medicine



- by the aggregation morphology. *J Ethnopharmacol* 2009; 123: 267–274.
- [16]Lv SW, Su H, Sun S, Guo YY, Liu T, Ping Y, et al. Isolation and characterization of nanometre aggregates from a bai-hu-tang decoction and their antipyretic effect. *Sci Rep* 2018; 8: 1–10.
- [17]Lin D, Du Q, Wang HQ, Gao GZ, Zhou JW, Ke LJ, et al. Antidiabetic micro-/nanoaggregates from ge-gen-qin-lian-tang decoction increase absorption of baicalin and cellular antioxidant activity in vitro. *Biomed Res Int* 2017; 2017: 9217912.
- [18]Zheng W, Sun GX, Chen JH, Li ZH, Zhang T, Wei GJ, et al. Inhibitory effects of *Coptidis Rhizoma* on the intestinal absorption and metabolism of *Scutellariae Radix*. *J Ethnopharmacol* 2021; 270: 113785.
- [19]Xiao SW, Liu C, Chen MJ, Zou JF, Zhang ZM, Cui X, et al. *Scutellariae radix* and *coptidis rhizoma* ameliorate glycolipid metabolism of type 2 diabetic rats by modulating gut microbiota and its metabolites. *Appl Microbiol Biot* 2020; 104: 303–317.
- [20]Hu ZP, Yang MY, Liu Y, Yang QY, Xie HY, Peng SH, et al. Effect of Huang-Lian Jie-Du decoction on glucose and lipid metabolism in type 2 diabetes mellitus: A systematic review and meta-analysis. *Front Pharmacol* 2021; 12: 648861.
- [21]Zhang ZW, Zhang NN, Li YM. Content Change of Main Chemical Composition Before and After Compatibility of *Scutellaria baicalensis* and *Coptis chinensis*. *Chin J Exp Tradit Med Form* 2012; 18: 58–62.
- [22]Wang JR, Tanaka T, Zhang H, Kouno I, Jiang Z H. Formation and conformation of baicalin – berberine and wogonoside – berberine complexes. *Chem Pharm Bull* 2012; 60: 706–711.
- [23]Li W, Song FR, Liu ZQ, Liu SY. Studies on change of chemical composition in *Coptis-Scute* herb couple by using HPCE and HPLC. *Acta Pharm Sin* 2008; 43: 191–194.
- [24]Li T, Wang PL, Guo WB, Huang XM, Tian XH, Wu GR, et al. Natural Berberine-Based Chinese Herb Medicine Assembled Nanostructures with Modified Antibacterial Application. *ACS Nano* 2019; 13: 6770–6781.
- [25]Cai XX, Weng QX, Lin JM, Chen GQ, Wang SY. Radix *Pseudostellariae* protein-curcumin nanocomplex: improvement on the stability, cellular uptake and antioxidant activity of curcumin. *Food Chem Toxicol* 2021; 151: 112110.
- [26]Bag BG, Dash SS. Hierarchical self-assembly of a renewable nanosized pentacyclic dihydroxy-triterpenoid betulin yielding flower-like architectures. *Langmuir* 2015; 31: 13664–13672.
- [27]Kumorek M, Minisy IM, Krunclová T, Voršiláková M, Vencliková K, Chánová EM, et al. pH-responsive and antibacterial properties of self-assembled multilayer films based on chitosan and tannic acid. *Mater Sci Eng C* 2020; 109: 110493.
- [28]Li Qk, Li JZ, Yu WK, Wang ZH, Li JW, Feng XJ, et al. De novo design of a pH-triggered self-assembled β -hairpin nanopeptide with the dual biological functions for antibacterial and entrapment. *J Nanobiotechnol* 2021; 19: 1–19.
- [29]Naskar J, Banerjee A. Concentration dependent transformation of oligopeptide based nanovesicles to nanotubes and an application of nanovesicles. *Chem – Asian J* 2009; 4: 1817–1823.
- [30]Liu J, Kim YT, Kwon YU. Hematite Thin Films with Various Nanoscopic Morphologies Through Control of Self-Assembly Structures. *Nanoscale Res Lett* 2015; 10: 1–10.
- [31]Von Staszewski M, Ruiz-Henestrosa VMP, Pilosof AMR. Green tea polyphenols- β -lactoglobulin nanocomplexes: Interfacial behavior, emulsification and oxidation stability of fish oil. *Food Hydrocoll* 2014; 35: 505–511.
- [32]Gao M, Yang YF, Bergfel A, Huang LL, Zheng L, Bowden TM. Self-assembly of cholesterol end-capped polymer micelles for controlled drug delivery. *J Nanobiotechnol* 2020; 18: 1–10.
- [33]Zhang M, Ye LL, Huang H, Cheng DD, Liu KX, Wu WB, et al. Micelles self-assembled by 3-O- β -d-glucopyranosyl latycodigenin enhance cell membrane permeability, promote antibiotic pulmonary targeting and improve anti-infective efficacy. *J Nanobiotechnol* 2020; 18: 1–15.
- [34]Wang YM, Wang J, Wang TS, Xu YS, Shi L, Wu YT, et al. Pod-Like Supramicelles with Multicompartment Hydrophobic Cores Prepared by Self-Assembly of Modified Chitosan. *Nano-micro Lett* 2016; 8: 151–156.
- [35]Zhai Y, Chai W, Cao WW, Sun ZP, Huang YD. Organogelators based on p-alkoxybenzamide and their self-assembling properties. *Front Chem Sci Eng* 2015; 9: 488–493.
- [36]Ghosh D, Farahani AD, Martin AD, Thordarson P, Damodaran KK. Unraveling the Self-Assembly Modes in Multicomponent Supramolecular Gels Using Single-Crystal X-ray Diffraction. *Chem Mater* 2020; 32: 3517–3527.
- [37]Smulders MMJ, Schenning APHJ, Meijer EW. Insight into the mechanisms of cooperative self-assembly: The “sergeants-and-soldiers” principle of chiral and achiral C₃-symmetrical discotic triamides. *J Am Chem Soc* 2008; 130: 606–611.
- [38]Roqanian S, Meratan AA, Ahmadian S, Shafizadeh M, Ghasemi A, Karami L. Polyphenols protect mitochondrial membrane against permeabilization induced by HEWL oligomers: Possible mechanism of action. *Int J Biol Macromol* 2017; 103: 709–720.
- [39]Guo NH, Wang CL, Shang C, You X, Zhang LY, Liu WB. Integrated study of the mechanism of tyrosinase inhibition by baicalin using kinetic, multispectroscopic and computational simulation analyses. *Int J Biol Macromol* 2018; 118: 57–68.
- [40]Gao YX, Hao J, Wu JD, Li Y, Lin Y, Hu J, et al. Cooperative supramolecular helical assembly of a pyridinium-tailored methyl glycyrrhetate. *Soft Matter* 2016; 12: 8979–8982.
- [41]Zhu GJ, Cheng SW, Hu Y, Li W, Mu JS. Synthesis and crystallization-driven solution self-assembly of PE-b-PMMA: controlling Micellar morphology through crystallization temperature and molar mass. *J Polym Res* 2020; 27: 1–11.
- [42]Huang RL, Wang YF, Qi W, Su RX, He ZM. Temperature-induced reversible self-assembly of diphenylalanine peptide and the structural transition from organogel to crystalline nanowires. *Nanoscale rRes Lett* 2014; 9: 1–9.
- [43]Jin J, Yang F, Li B, Liu D, Wu LH, Li Y, et al. Temperature-regulated self-assembly of lipids at free bubbles interface: A green and simple method to prepare micro/nano bubbles. *Nano Res* 2020; 13: 999–1007.
- [44]Frassinetti S, Falleni A, Del Carratore R. Effect of itraconazole on *Staphylococcus aureus* biofilm and extracellular vesicles formation. *Microb Pathogenesis* 2020; 147: 104267.
- [45]Tang JN, Kang MS, Chen HC, Shi XM, Zhou R, Chen J, et al. The staphylococcal nuclease prevents biofilm formation in *Staphylococcus aureus* and other biofilm-forming bacteria. *Sci China Life Sci* 2011; 54: 863–869.



- [46]Zhang JM, Liao W, He YX, He Y, Yan D, Fu CM. Study on intestinal absorption and pharmacokinetic characterization of diester diterpenoid alkaloids in precipitation derived from Fuzi-Gancao herb-pair decoction for its potential interaction mechanism investigation. *J Ethnopharmacol* 2013; 147: 128–135.
- [47]Yan R, Wang Y, Shen WJ, Liu YP, Di X. Comparative pharmacokinetics of dehydroevodiamine and coptisine in rat plasma after oral administration of single herbs and Zuojinwan prescription. *Fitoterapia* 2011; 82: 1152–1159.
- [48]Zhan JYX, Zheng KYZ, Zhang WL, Chen JP, Yao P, Bi CWC, et al. Identification of Angelica oil as a suppressor for the biological properties of Danggui Buxue tang: A Chinese herbal decoction composes of Astragali Radix and Angelica Sinensis Radix. *J Ethnopharmacol* 2014; 154: 825–831.